

11-29-2005

Conduction-band tight-binding description for Si applied to P donors

A. S. Martins

Universidade Federal Fluminense

Timothy B. Boykin

The University of Alabama, Huntsville

Gerhard Klimeck

Purdue University - Main Campus, gekco@purdue.edu

Belita Koiller

Universidade Federal do Rio de Janeiro

Follow this and additional works at: <http://docs.lib.purdue.edu/nanodocs>

Martins, A. S.; Boykin, Timothy B.; Klimeck, Gerhard; and Koiller, Belita, "Conduction-band tight-binding description for Si applied to P donors" (2005). *Other Nanotechnology Publications*. Paper 108.
<http://docs.lib.purdue.edu/nanodocs/108>

This document has been made available through Purdue e-Pubs, a service of the Purdue University Libraries. Please contact epubs@purdue.edu for additional information.

Conduction-band tight-binding description for Si applied to P donors

A. S. Martins,¹ Timothy B. Boykin,² Gerhard Klimeck,³ and Belita Koiller⁴

¹*Instituto de Física, Universidade Federal Fluminense, 24210-340, Niteroi-RJ, Brazil*

²*Department of Electrical and Computer Engineering, The University of Alabama in Huntsville, Huntsville, Alabama 35899, USA*

³*Network for Computational Nanotechnology, Electrical and Computer Engineering, Purdue University, West Lafayette, Indiana 47907, USA*

and Jet Propulsion Laboratory, California Institute of Technology, Pasadena, California 91109, USA

⁴*Instituto de Física, Universidade Federal do Rio de Janeiro, Cx.P. 68.528, 21945-970, RJ, Brazil*

(Received 6 May 2005; revised manuscript received 21 July 2005; published 29 November 2005)

A tight-binding parametrization for silicon, optimized to correctly reproduce effective masses as well as the reciprocal space positions of the conduction-band minima, is presented. The reliability of the proposed parametrization is assessed by performing systematic comparisons between the descriptions of donor impurities in Si using this parametrization and previously reported ones. The spectral decomposition of the donor wave function demonstrates the importance of incorporating full band effects for a reliable representation, and that an incomplete real space description results from a truncated reciprocal space expansion as proposed within the effective mass theory.

DOI: [10.1103/PhysRevB.72.193204](https://doi.org/10.1103/PhysRevB.72.193204)

PACS number(s): 71.15.Ap, 71.55.Cn, 03.67.Lx

Advances in semiconductor device fabrication, particularly Si-based devices, have benefited from the progressive miniaturization and integration of their constituent parts, including detailed control of the doping process. The theoretical approach utilized for device modeling should be able to resolve charge-density variations on an atomic scale, and in this respect tight-binding (TB) models are particularly adequate, as they provide atomistic descriptions of structural and electronic properties of solids.¹ Since the pioneering work of Slater and Koster,² TB is conceived as an empirical method, where orbital energies and hoppings are parameters to be adjusted in order to reproduce relevant properties in the band structure of the solid. TB methods rely on the choice of a suitable parametrization of the Hamiltonian, which includes the choice of a basis set, range of hopping coupling, etc. For the group IV and III–V semiconductors one might expect that the minimal sp^3 basis with first-neighbors coupling should suffice to describe the essential physics. However, this model is not able to reproduce the gaps of the indirect gap materials like Si and AlAs.³ A simple scheme to correct this deficiency consists in introducing an excited s -like orbital, s^* , to improve the description of the conduction band (CB).⁴ Another limitation of first-neighbor models based on s and p orbitals alone is that they predict an infinite value of the transverse effective mass at the X point. This anomaly may be overcome either by adding the five d orbitals in the first-neighbor basis set,^{5,6} or by inclusion of second-neighbor (2nn) interactions in the sp^3s^* model.⁷

Comparison between the different TB parametrizations for Si available in the literature shows that the one that best reproduces the relevant bulk material properties is the one proposed by Klimeck *et al.*,⁸ based on the first and second-neighbors sp^3s^* model. The reciprocal space position of the CB minima, however, is not well fitted. Silicon is an indirect gap material, with 6 CB minima along the equivalent Δ lines, 85% of the way between Γ and X . In Ref. 8, a genetic algorithm (GA) fitting was adopted, and the target position for the minima was considered as 75% between Γ and X . For some applications^{6,9} it is known that a shift in the position of

the CB minimum may lead to unsatisfactory results. We present here an improved parametrization, also obtained through the GA methodology,⁸ reproducing the correct positions of the CB edges.

GA-based optimization employs stochastic methods which do not require constraints on continuity of solution space. In the case considered here, the TB parameters are varied in order to get an optimal set that reproduces given material properties, denoted as target values. Details on the method are discussed in Ref. 8: We refer to the parametrization published there as P075, and to the one proposed here as P085. Both parametrizations give the k -space positions of the six band minima at six equivalent points along Δ lines, with the position of the minimum at $\Delta_{min}=0.75(2\pi/a_{Si})$ for P075 and $\Delta_{min}=0.85(2\pi/a_{Si})$ for P085, where $a_{Si}=5.431 \text{ \AA}$ is the conventional cubic lattice parameter for Si. Table I presents the TB parameters for Si for both parametrizations. The main difference between them consists in allowing nonzero 2nn hoppings $V_{ss^*}(110)$ and $V_{s^*s^*}(110)$ in the optimization set for P085. All 2nn hoppings are consistently smaller than the first neighbors. The 2nn hopping parameters were determined to adjust the finer details of the target properties, and were not constrained to have values or signs expected from physical considerations.²

The input and the calculated properties are presented in Table II, where the first column shows the material properties to be represented by the TB model and the second column shows the corresponding experimental values.¹⁰ These constitute the input targets in the GA code. The remaining columns give the calculated properties and the respective deviations from the experimental targets for P075 and P085, as well as for a recently proposed first-neighbor $sp^3d^5s^*$ parametrization, which we denote by P1nn.⁶ We note from Table II that the P075 and P085 parametrizations give consistently better agreement with the target values than the P1nn parametrization. This statement cannot be generalized as a fundamental advantage of the second-neighbor sp^3s^* model over the nearest-neighbor $sp^3d^5s^*$ model. The P1nn set⁶ satisfies additional requirements beyond bulk behavior properties.

TABLE I. Parameters for the TB models (in eV).

Parameter	P075	P085
$E_s(000)$	-4.81341	-4.848054
$E_p(000)$	1.77563	1.787118
$E_{s^*}(000)$	6.61342	5.608014
$V_{ss}\left(\frac{111}{222}\right)$	-8.33255	-8.259704
$V_{xx}\left(\frac{111}{222}\right)$	1.69916	1.697556
$V_{xy}\left(\frac{111}{222}\right)$	5.29091	5.351079
$V_{sp}\left(\frac{111}{222}\right)$	5.86140	5.822197
$V_{s^*p}\left(\frac{111}{222}\right)$	4.88308	4.864480
λ_{SO}	0.04503	0.014905
$V_{ss}(110)$	0.01591	0.029958
$V_{s^*s^*}(110)$	0.00000	0.191517
$V_{ss^*}(110)$	0.00000	0.007036
$V_{sx}(110)$	0.08002	0.161749
$V_{sx}(011)$	1.31699	0.885988
$V_{s^*x}(110)$	-0.00579	-0.095653
$V_{s^*x}(011)$	0.50103	0.966257
$V_{xt}(110)$	0.00762	0.037296
$V_{xt}(011)$	-0.10662	-0.132810
$V_{xy}(110)$	0.55067	0.619876
$V_{xy}(011)$	-2.27784	-2.496288

On-going work indicates that the $sp^3d^5s^*$ model can be fit to match the Si bulk properties just as well as the second-neighbor sp^3s^* model. The primary advantage of the nearest-neighbor $sp^3d^5s^*$ model is its straightforward incorporation of strain distortions.¹¹ In the donor description below, no strain distortions are considered, and the second-neighbor model P085 provides an unprecedented representation of the Si CB.

The reliability of TB sp^3s^* second-neighbors parametrizations has been recently verified by studies of shallow donors in GaAs¹² and in Si.¹³ We perform the same kind of study here, and discuss the effect of the CB minimum position in different aspects of the donor problem. We write the Hamiltonian for the impurity problem as¹⁴ $H = \sum_{ij} \sum_{\mu\nu} h_{ij}^{\mu\nu} c_{i\mu}^\dagger c_{j\nu} + \sum_{i,\nu} U(R_i) c_{i\nu}^\dagger c_{i\nu}$ where i and j label the atomic sites, μ and ν denote the atomic orbitals and R_i is the distance between site i and the impurity site. The impurity potential is taken as a screened Coulomb potential, $U(R_i) = -e^2/(\epsilon R_i)$ ($\epsilon = 12.1$ for Si). At the impurity site it is assigned the value $U(R_i=0) = -U_0$, a parameter describing central cell effects characteristic of the substitutional species, and taken here as an adjustable parameter. We do not include spin-orbit corrections in the present calculations.

The eigenstates of H are determined for a system where a single impurity is placed in a cubic supercell containing $N = 8L^3$ atoms in the diamond structure, where L is the length

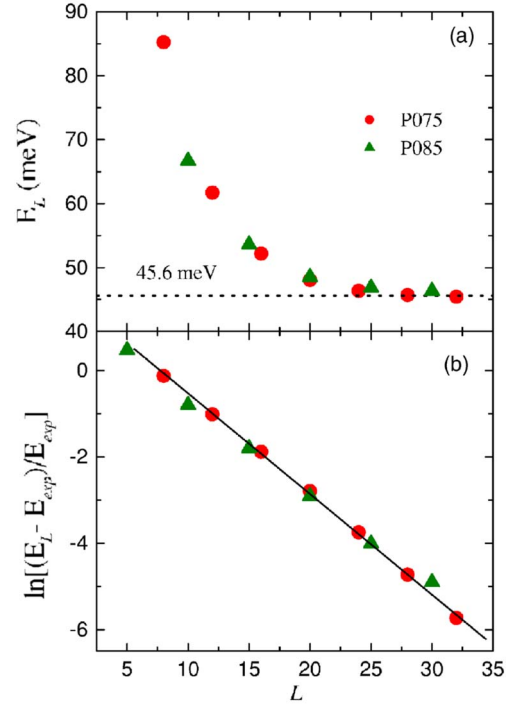


FIG. 1. (Color online) (a) Convergence of the donor ground state binding energy towards the experimental value (dotted line gives $E_{exp} = 45.6$ meV) with the supercell size L , for $U_0 = U_P$, namely 1.48 eV and 1.26 eV for P075 and P085, respectively. (b) Same data plotted as $\ln[(E_L - E_{exp})/E_{exp}]$ vs L . The linear behavior (the line is a best fit for all data points) indicates that the convergence of the binding energy with the supercell size L follows the same exponential law for both parametrizations.

of the supercell edge in units of a_{Si} . We adopt periodic boundary conditions, and large supercells¹² (up to 10^6 atoms) were treated within a variational scheme^{15,16} where the ground state wavefunction and binding energy E_L are obtained by minimizing $\langle \Psi | (H - \epsilon_{ref})^2 | \Psi \rangle$. The reference energy ϵ_{ref} is chosen within the gap, nearest to the CB edge.

The eigenfunctions of H in the basis of atomiclike orbitals are written as $|\Psi_{TB}(\mathbf{r})\rangle = \sum_{i\nu} a_{i\nu} |\phi_\nu(\mathbf{r} - \mathbf{R}_i)\rangle$, where the expansion coefficients $a_{i\nu}$ give the probability amplitude of finding the electron in the orbital ν at site \mathbf{R}_i . The overall charge distribution is conveniently described through the TB envelope function squared,¹⁷

$$|\Psi_{EF}(\mathbf{R}_i)|^2 = \sum_{\nu} |a_{i\nu}|^2. \quad (1)$$

In Fig. 1, a convergence study of the donor ground state binding energy as a function of the supercell size L is presented for P075 and P085. One can observe in Fig. 1(a) that for supercell sizes $L > 25$ the calculated binding energies reproduce the experimental value ($E_{exp} = 45.6$ meV) taking $U_0 = 1.48$ and $U_0 = 1.26$ eV for P075 and P085, respectively. We denote these values by U_P , as they are determined by tuning the on-site potential $-U_0$ in order to give the converged value of E_b in agreement with experiment for P donors in Si. Figure 1(b) presents a plot of $\ln[(E_L - E_{exp})/E_{exp}]$ vs L . The linear behavior obtained here indi-

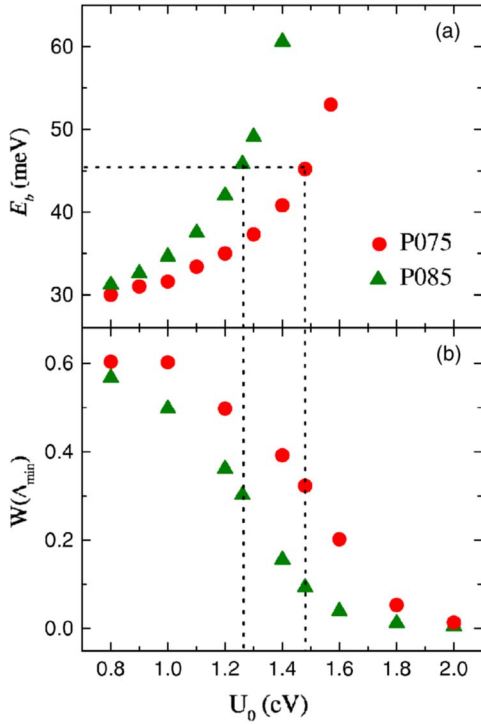


FIG. 2. (Color online) (a) Binding energy of the ground state as a function of the on-site perturbation strength U_0 . The dotted lines indicate the value $U_0 = U_p$ that reproduces the experimental Si:P A_1 state binding energy. (b) Total spectral weight at the CB edges for the ground impurity state.

ates *the same* exponential convergence of E_L to the experimental value for both parametrizations: $E_L \sim E_{exp} + \tilde{E}e^{-L/\lambda}$.

We determine the first excited state energy¹³ by varying the value of ε_{ref} in $\langle \Psi | (H - \varepsilon_{ref})^2 | \Psi \rangle$. Keeping $U_0 = 1.26$ eV, we obtain the binding energy of the first excited state to be

30.2 meV, in good agreement with the P075 result, 32.4 meV.

The behavior of the binding energy with U_0 is presented in Fig. 2(a), where the dotted lines indicate the value of U_p for each parametrization leading to $E_b = E_{exp}$. As noted in Ref. 13, in the weak perturbation limit the binding energies converge to the effective mass theory (EMT) prediction in its simplest formulation¹⁸ (single-valley approximation), ~ 30 meV. It is interesting that this behavior is the same for both parametrizations. As U_0 increases, P085 tends to give higher binding energies than P075, resulting in a smaller value of U_p for P085.

One can also characterize the donor ground state by its orbital averaged spectral weight¹⁷ at $\mathbf{k} = \Delta_{min}$, $W(\Delta_{min}) = (2/N) \sum_{\mu=1}^6 \sum_{ij} e^{i\mathbf{k}_{\mu} \cdot (\mathbf{R}_i - \mathbf{R}_j)} a_{i\mu} a_{j\nu}$, plotted in Fig. 2(b) as a function of U_0 . The EMT approach presumes that $W(\Delta_{min}) \sim 1$, allowing the donor state to be well described in a basis of Bloch states at the CB-edge \mathbf{k} points. However, one can notice in Fig. 2(b) that this is not the case: Even for the smallest values of U_0 the spectral weights at Δ_{min} are well below saturation (one) for both parametrizations, implying that an incomplete description may result from EMT in this case. The spectral weight at U_p is 0.32 for P075 and 0.30 for P085. These relatively low spectral weights indicate that multiple \mathbf{k} points, other than those corresponding to the six CB edges of Si, contribute to the donor wave function expansion within any reciprocal-space based approach.

Within single-valley EMT the ground state for donors in Si is sixfold degenerate.¹⁸ Valley-orbit interactions¹⁹ lead to a nondegenerate ground state wave function of A_1 symmetry,

$$\psi(\mathbf{r}) = \frac{1}{\sqrt{6}} \sum_{\mu=1}^6 F_{\mu}(\mathbf{r}) u_{\mu}(\mathbf{r}) e^{i\mathbf{k}_{\mu} \cdot \mathbf{r}}, \quad (2)$$

where $\phi_{\mu}(\mathbf{r}) = u_{\mu}(\mathbf{r}) e^{i\mathbf{k}_{\mu} \cdot \mathbf{r}}$ are the pertinent Bloch wave functions, and the envelope functions are given by $F_{\mu}(\mathbf{r})$

TABLE II. Optimization targets and optimized material properties for the P075, P085, and P1nn models. Except for Δ_{min} , which is specific for different models, the target values correspond to experimental data given in Ref. 10.

Property	Target	P075	%dev	P085	%dev	P1nn	%dev
Δ_{min}	0.750	0.758	1.067				
	0.850			0.8480	-0.235	0.813	-4.35
E_c^{Γ}	3.350	3.353	0.089	3.350	-0.013	3.399	1.44
$E_c^{\Delta_{min}}$	1.130	1.129	-0.050	1.130	-0.042	1.131	0.09
m_{Xl}^*	0.916	0.916	-0.030	0.916	0.050	0.891	-2.73
m_{Xt}^*	0.191	0.191	0.020	0.191	0.007	0.201	-5.23
$m_{lh}^*[001]$	-0.204	-0.198	3.082	-0.204	-0.060	-0.214	-4.90
$m_{lh}^*[011]$	-0.147	-0.146	0.525	-0.148	-0.568	-0.152	-3.40
$m_{lh}^*[111]$	-0.139	-0.139	0.395	-0.140	-0.610	-0.144	-3.60
$m_{hh}^*[001]$	-0.275	-0.285	-3.643	-0.277	-0.786	-0.276	-0.36
$m_{hh}^*[011]$	-0.579	-0.581	-0.338	-0.574	0.869	-0.581	-0.34
$m_{hh}^*[111]$	-0.738	-0.737	0.119	-0.727	1.466	-0.734	0.54
m_{so}^*	-0.234	-0.237	-1.487	-0.239	-2.162	-0.246	-5.13
Δ_{so}	0.015	0.145	-0.067	0.015	0.030	0.016	4.90

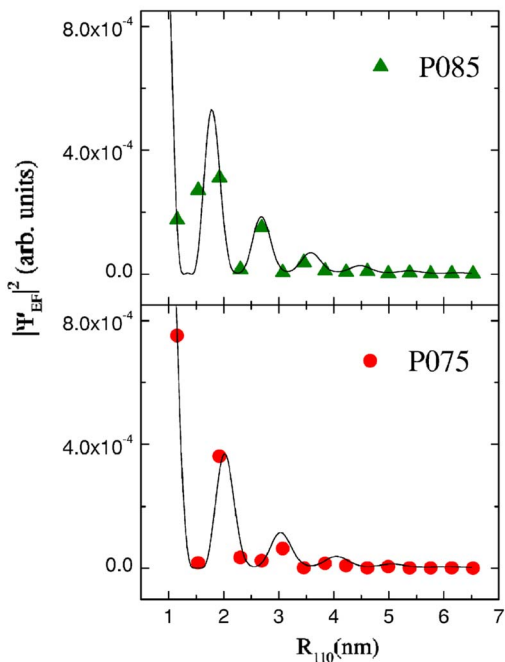


FIG. 3. (Color online) TB envelope function squared for the donor ground state along the [110] direction. The lines are the corresponding effective mass $|\psi|^2$ results.

$= (1/\sqrt{\pi a^2 b}) e^{-[(x^2+y^2)/a^2+z^2/b^2]^{1/2}}$ for $\mu=z$ and equivalently for the other μ values. The effective Bohr radii for Si are $a=2.51$ nm and $b=1.44$ nm.⁹ Figure 3 presents a comparison between the TB envelope function calculated from (1) along the [110] direction, for both P075 and P085 parametrizations (data points) with the corresponding EMT results obtained from (2) (solid lines), with a and b are given above, but with a different normalization to conciliate the TB and EMT wave functions on the same scale. The values of \mathbf{k}_μ used in (2) are consistent with the respective reciprocal space location of the CB minima. Note that the oscillatory behavior due to interference among the plane-wave parts of the six ϕ_μ is well captured by the TB envelope function. The period of the

oscillations is different for P075 and P085, as given by the corresponding wave vectors.

Good agreement between TB and EMT is restricted to distances from the impurity site larger than ~ 1 nm. This means that at large distances the EMT expansion of the donor wavefunction in only six \mathbf{k} points, as given in Eq. (2), is capable of reproducing its main features (except for normalization, of course). Closer to the impurity, particularly at the impurity site, the TB results become much larger than the EMT prediction.

The wave functions obtained from P085 and P075 agree reasonably well in the central cell region. One way to quantify this agreement is through the probability to find the donor electron inside of a sphere of radius R_c : $Q(R_c) = \sum_{R \leq R_c} |a_{i\nu}(R)|^2$. Taking for R_c the 2nn distance, the ratio of $Q(R_c)$ obtained from the two parametrizations is $Q_{P085}(R_c)/Q_{P075}(R_c) = 1.15$.

In summary, we find good agreement between the results obtained within P085 and P075 for (i) the exponential convergence law for the ground state binding energy with supercell size, (ii) the binding energy of the first excited state, (iii) the spectral weight of the ground state wave function at Δ_{min} , (iv) the probability that the donor electron is within the central cell up to the impurity's 2nn. Both parametrizations also capture the donor wave function oscillations predicted within EMT; the main difference regards the period of the oscillations. In applications where the quantitative aspects of the oscillatory behavior of the wave function is important, the P085 parametrization is thus capable of providing a better description. The importance to represent the P impurity wave function in a full band, atomistic representation is demonstrated through its spectral decomposition, and by direct comparison between the TB results and EMT.

We thank F.J. Ribeiro for fruitful discussions. B.K. acknowledges the hospitality of CMTC at the University of Maryland. This work was partially supported in Brazil by FAPERJ, CAPES, FUJB, Instituto do Milênio de Nanociências/MCT, and at the Jet Propulsion Laboratory, Caltech by NASA. Funding for G.K. was provided by JPL, NASA-ESTO, ARDA, ONR, and NSF.

¹A. Di Carlo, *Semicond. Sci. Technol.* **18**, R1 (2003), and references therein.

²J. C. Slater and G. F. Koster, *Phys. Rev.* **94**, 1498 (1954).

³D. J. Chadi and M. L. Cohen, *Phys. Status Solidi B* **68**, 405 (1975).

⁴P. Vogl, H. P. Hjalmarson, and J. D. Dow, *J. Phys. Chem. Solids* **44**, 365 (1983).

⁵J.-M. Jancu *et al.*, *Phys. Rev. B* **57**, 6493 (1998).

⁶T. B. Boykin, G. Klimeck, and F. Oyafuso, *Phys. Rev. B* **69**, 115201 (2004).

⁷T. B. Boykin, *Phys. Rev. B* **56**, 9613 (1997).

⁸G. Klimeck *et al.*, *Superlattices Microstruct.* **27**, 77 (2000).

⁹B. Koiller, X. Hu, and S. Das Sarma, *Phys. Rev. Lett.* **88**, 027903 (2002).

¹⁰O. Madelung, *Semiconductor-Basic Data* (Springer, Berlin, 1996).

¹¹T. B. Boykin *et al.*, *Phys. Rev. B* **66**, 125207 (2002).

¹²A. S. Martins *et al.*, *Phys. Rev. B* **65**, 245205 (2002).

¹³A. S. Martins, R. B. Capaz, and B. Koiller, *Phys. Rev. B* **69**, 085320 (2004).

¹⁴J. G. Menchero *et al.*, *Phys. Rev. B* **59**, 2722 (1999).

¹⁵R. B. Capaz *et al.*, *J. Appl. Phys.* **74**, 5531 (1993).

¹⁶L. W. Wang and A. Zunger, *J. Chem. Phys.* **100**, 2394 (1994).

¹⁷T. G. Dargam, R. B. Capaz, and B. Koiller, *Phys. Rev. B* **56**, 9625 (1997).

¹⁸W. Kohn, *Solid State Physics Series* (Academic, New York, 1957), Vol. 5.

¹⁹A. Baldereschi, *Phys. Rev. B* **1**, 4673 (1970).